Two Classes of β Pleated-Sheet Conformation in Poly(L-tyrosine): A Model for Tertiary Structure in Native Proteins[†]

Henry E. Auer* and Roy P. McKnight[‡]

ABSTRACT: Poly(L-tyrosine) generates the antiparallel β-sheet conformation at low ionization in aqueous solution. In this work the properties of three samples of $(Tyr)_n$, numbered 1–3 in order of increasing degree of polymerization, were investigated at solute concentrations low enough to form only intramolecular (i.e., nonaggregated) β structures. It was concluded that two classes of β structure are formed by $(Tyr)_n$ in solution, with samples 1 and 2 comprising class I and sample 3 representing class II. This finding is based on distinctions observed in the sedimentation coefficient and in the far-ultraviolet circular dichroism spectra, ascribed to the side-chain chromophore. Furthermore, distinctions in the entropy change for the β-disordered chain transition, the breadth of the transition, and the electrostatic potential in the ordered state, based on spectrophotometric-potentiometric titrations on samples 1 and 3, have already been reported [McKnight, R. P., and Auer, H. E. (1976), *Macromolecules 9*, 939–944]. A comparison of the experimental frictional ratios with values calculated from a variety of model ellipsoids of revolution reveals that the hydrodynamic properties of samples 1 and 2 are consistent only with very anisotropic model particles; it is likely that they have only a few polypeptide chain segments folded into long, open-sheet β structures. The properties of sample 3, on the other hand, suggest that it adopts a more compact shape, and it is proposed that the β sheet in this particle is folded over onto itself to generate a double-layered structure. If so this may represent the first instance of prototypical tertiary structure generated in a system as simple as a β-forming homopoly-(amino acid). The distinctions observed for all other properties studied are consistent with these proposed hydrodynamic models. When sample 3 is transferred from sodium buffer, in which the properties summarized above are observed, to tetramethylammonium buffer, its behavior changes to that characteristic of the low-DP class. Dialysis back to sodium medium largely restores the original properties. This shows that the development of the folded β structure in $(Tyr)_n$ is readily modulated by varying experimentally accessible parameters.

Poly(L-tyrosine) in aqueous solution is known to form the β pleated sheet conformation at low ionization (Patrone et al., 1970; Conio et al., 1971; Senior et al., 1971; Patton and Auer, 1975). It has been shown that when the concentration is sufficiently low the β structure forms intramolecularly; that is, it is not aggregated (Patton and Auer, 1975), in contrast to the β form of other homopoly(amino acids) such as poly(L-lysine) (Hartman et al., 1974). This is one of the few instances of an intramolecular pleated-sheet structure in a high-molecular-weight poly(amino acid) and as such merits further study as a model for the β conformation in native proteins. We have already shown, for example, that the hydrodynamic properties of a sample of $(Tyr)_n$ having a relatively high degree of polymerization (DP)[1] are consistent with a compact particle which may be formed by a single pleated sheet which is folded over on itself (Patton and Auer, 1975). Further work revealed that the kinetics of formation of the pleated-sheet structure are independent of polymer concentration and conform to a two-step first-order process (Auer and Patton, 1976). Subsequently, the thermodynamic parameters for the β-disordered chain conformational transition were found to depend on the DP of the sample, as do the breadth of the transition and the dependence of the electrostatic potential in the ordered state on the degree of ionization, α, of the side chain (McKnight and Auer, 1976). It was suggested that these distinctions were due to a molecular-weight-dependent difference in the nature of the pleated-sheet structure adopted in solution.

In order better to characterize this phenomenon, we have carried out further hydrodynamic and spectroscopic studies on this system. The results reported in this paper confirm and extend our original observations. Two distinct classes of behavior were found, and under certain circumstances the same sample could be made to interconvert between them. Models consistent with the observed distinctions are proposed for the two classes of β structure found. From this study a more detailed understanding of the pleated-sheet conformation in simple model systems and globular proteins emerges.

Materials and Methods

Three samples of $(Tyr)_n$ were used in this work. Their molecular weights are listed in Table I. The samples from Sigma Chemical Co. and from Pilot Chemicals Division, New England Nuclear Corp., were the same as the ones used in our previous study (McKnight and Auer, 1976). During the course of this work, lasting over 2 years, it was observed that, in our hands, the DP of these samples decreased with time, even though they were stored at -15 °C, being withdrawn only occasionally for preparation of solutions at room temperature. The molecular weight of the Pilot sample began at 99 700 and that of the Sigma sample was originally 27 300 (McKnight and

* To whom correspondence should be addressed at the Department of Biochemistry, The Medical College of Wisconsin, Milwaukee, Wis. 53226.

‡ Present Address: Clinical Chemistry Laboratories, Department of Laboratory Medicine, University Hospital SB-10, University of Washington, Seattle, Wash. 98195.

[1] Abbreviations used: CD, circular dichroism; DP, degree of polymerization; TMA, tetramethylammonium cation; TMAP, TMA phosphate; α, degree of ionization of the side chain.

TABLE I: Molecular Weights of Samples of Poly(L-tyrosine).

designation	source	mol wt[a]	DP
1	Sigma	16 700	104
2	Schwarz/Mann	63 800	390
3	Pilot	72 700	445

[a] Determined at high ionization (disordered state) in 0.01 M sodium phosphate by equilibrium ultracentrifugation, using a value for the partial specific volume of 0.71 cm³ g⁻¹ (Cohn and Edsall, 1943).

Auer, 1976). Strictly speaking, therefore, the samples used in the latter work and in the present study are not identical. Their distinctive properties, however, remained unchanged during the course of this work. The third sample was from Schwarz/ Mann. The concentration of $(Tyr)_n$ was kept at about 2×10^{-4} M in order to minimize the process of aggregation which occurs at low ionization. Solutions were generally buffered with 0.01 M phosphate. Sodium phosphate was prepared in a routine manner. Tetramethylammonium phosphate was prepared from standardized phosphoric acid by neutralizing with TMA-OH (Eastman Organic Chemical).

Experimental procedures were similar to those reported earlier (Patton and Auer, 1975; McKnight and Auer, 1976). In titrating samples from high ionization to lower pH, sufficient time was allowed for the transformation to the β structure to be completed (Auer and Patton, 1976). Powdered samples for infrared mulls were prepared by lyophilization after being injected slowly into vials precooled in a dry ice–acetone bath. Thus, the time required for freezing was reduced to 2–3 s. Unless otherwise noted, experiments were conducted at 20 °C.

Results

Sodium Phosphate Medium. The β-disordered chain transformation for a sample of $(Tyr)_n$ closely similar to sample 3 has been thoroughly characterized by Patton and Auer (1975). Infrared spectra clearly identified the ordered state as the antiparallel pleated-sheet conformation. Sharp changes were observed in the sedimentation coefficient $s_{20,w}$ and in the molar ellipticity $[\theta]_{227}$ as the pH was changed, concomitant with the transformation of the infrared spectra from those characteristic of the disordered state to those typical of the β structure. A further demonstration of this phenomenon at the lower ionic strength used in this work may be found in the pH dependence of other properties sensitive to the conformational transition. Circular dichroism spectra of sample 3 in the 230-nm region, attributed to the ^1L_a transition of the phenol chromophore, and in the 200-nm region, attributed to the ^1B transitions (Hooker and Schellman, 1970), are shown in Figure 1, bottom. A large increase in intensity is found at 201 nm as the conformation passes from the disordered to the ordered state, in addition to the change at 227 nm previously reported (Patton and Auer, 1975). The change in the intensity of the 201-nm band with pH is shown in Figure 2, together with a Henderson–Hasselbalch plot of titration data obtained for this sample during the course of our earlier work (McKnight and Auer, 1976). The Henderson–Hasselbalch plot depicts the pH dependence of the titration curve in a striking fashion, for the transition from the titration of the disordered state to that of the β conformation is clearly manifested. It is apparent from Figure 2 that the CD titration and the potentiometric titration change sharply over the same pH range, reflecting the conformational transformation occurring in the sample. It is important to note that these effects appear to be independent of
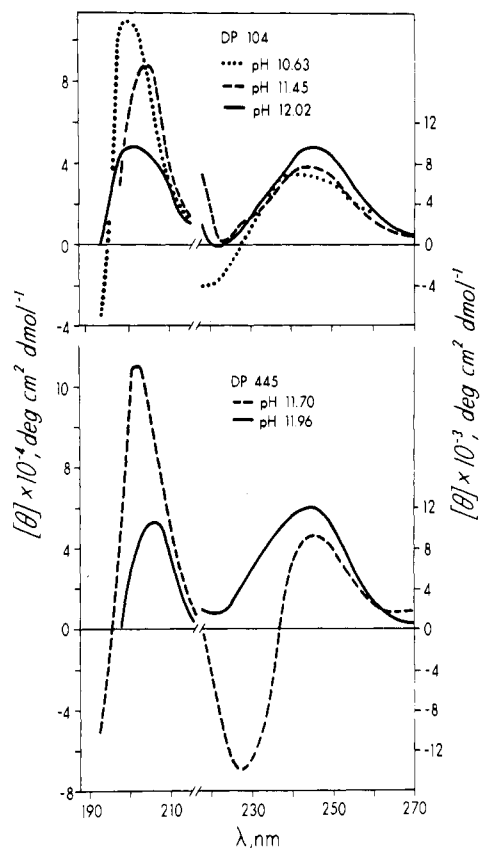

FIGURE 1: CD spectra of poly(L-tyrosine) in 0.01 M sodium phosphate: Top, sample 1; bottom, sample 3.
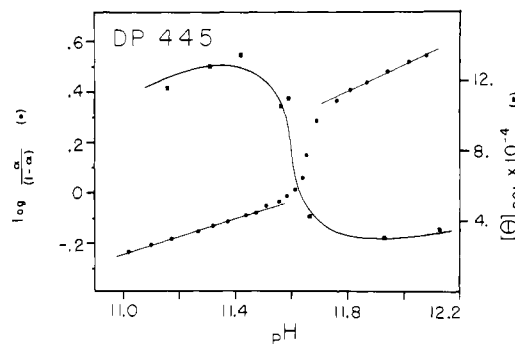

FIGURE 2: pH dependence of properties of sample 3: (●) spectrophotometric–potentiometric titration in 0.01 M sodium borate buffer, presented as a Henderson–Hasselbalch plot; (■) pH dependence of the molar ellipticity in 0.01 M sodium phosphate, in the region of the ^1B bands.

the change in ambient conditions from 0.16 M Na⁺, 25 °C (Patton and Auer, 1975), to 0.02 M Na⁺, 20 °C.

Evidence for the occurrence of an order–disorder transformation for sample 1 was presented by McKnight and Auer (1976), where the Zimm–Rice plots of the potentiometric titrations manifested the typical form for such a phenomenon. In order to identify the nature of the transition, infrared spectra in the region of the amide I band were recorded for sample 1 on mulls of lyophilized $(Tyr)_n$ prepared from solutions of known pH. The results, shown in Figure 3, closely resemble the spectra observed for $(Tyr)_n$ of higher DP obtained by Patton and Auer (1975). As the pH is lowered, the spectra change from those characteristic of the disordered state (a, b, $\nu = 1655$ cm⁻¹) to those characteristic of the antiparallel β pleated-sheet conformation (d, e, $\nu = 1629$ and 1696 cm⁻¹; Moore and Krimm, 1976b; Chirgadze and Nevskaya, 1976a).
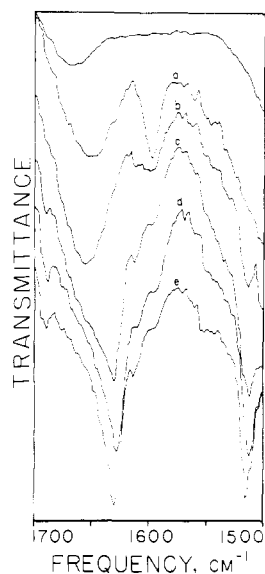
FIGURE 3: Infrared spectra of mulls of sample 1 lyophilized from 0.01 M sodium phosphate, using ordinate expansions of 5×. The spectrum at the top is that of a buffer blank treated in the same way as the samples: a, pH 12.41; b, pH 12.10; c, pH 11.82; d, pH 11.28; e, pH 10.94.
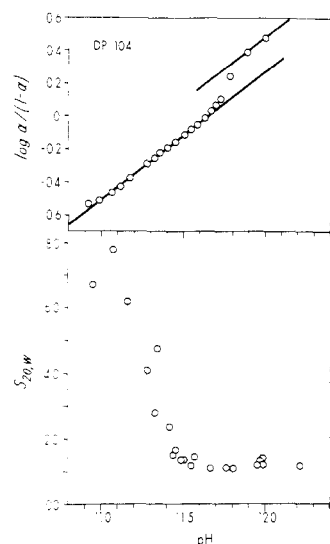

FIGURE 4: pH dependence of properties of sample 1 in 0.01 M sodium phosphate: top, Henderson–Hasselbalch plot of spectrophotometric-potentiometric titration (data from McKnight and Auer, 1976); bottom, sedimentation coefficient.
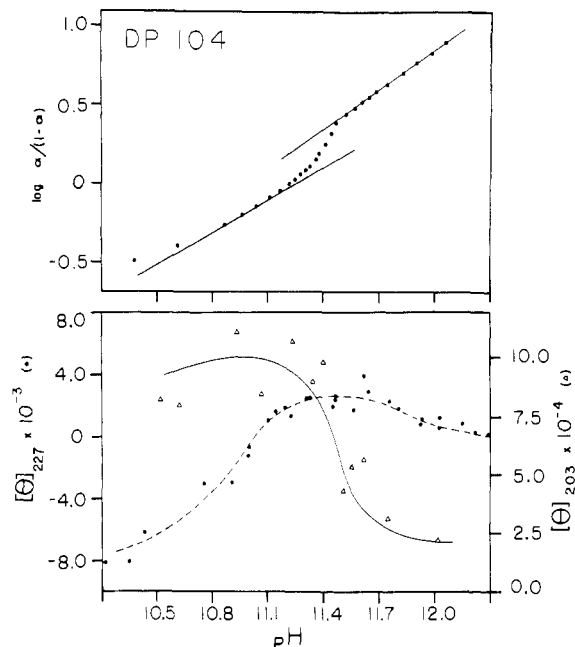

FIGURE 5: pH dependence of properties of sample 1 in 0.01 M sodium phosphate at 25 °C: top, Henderson–Hasselbalch plot of spectrophoto-metric–potentiometric titration (data from McKnight and Auer, 1976); bottom, molar ellipticity in the regions of the ^{1}B (△) and ^{1}L$_a$ (●) bands.

Spectrum c manifests contributions from both spectral forms, indicating that this pH falls within the range of the conformational transition. It may be concluded that the ordered state for sample 1 is the same as that found for sample 3.

CD spectra of sample 1 are shown in Figure 1, top. In spite of the fact that the ordered state is a β conformation, the CD spectrum of the intramolecular β state (pH 11.45) shows no significant change in the region of the ^{1}L$_a$ band from that found in the disordered state. Specifically, the intense negative extremum at 227 nm found with sample 3 is absent. Only at considerably lower pH values (10.63), at which aggregation has set in (see below), does weak negative intensity appear at about 220 nm. In contrast, the CD spectral changes which occur in the range of the ^{1}B band as the pH is altered apparently do reflect the β-disordered chain transformation more accurately. The intensity increases considerably as the pH is lowered to the region where the β form is prevalent but does

not attain the intensity observed with sample 3. Further decrease in pH produces a slight shift in peak position.

The Henderson–Hasselbalch plot for the potentiometric titration of sample 1, drawn from data obtained by McKnight and Auer (1976), is shown in Figure 4, together with the dependence of $s_{20,w}$ for this sample. The break in the Henderson–Hasselbalch curve occurs in the same pH range as the β-disordered chain transformation, as may be seen by referring to the infrared spectra of Figure 3. Nevertheless, no change in $s_{20,w}$ is observed in this pH range, within the limits of detection. This too is in contrast to the case of sample 3, where sharp changes in $s_{20,w}$ were obtained as the conformational change occurs (Patton and Auer, 1975). As the pH is decreased further, the values of $s_{20,w}$ increase many fold to magnitudes much larger than are possible for a particle of this molecular weight. This increase therefore must be ascribed to aggregation of molecules in the pleated-sheet conformation at low values of α.

Figure 5 shows the pH dependence of the molar ellipticity in the ^{1}L$_a$ and ^{1}B bands for sample 1 at 25 °C, together with a Henderson–Hasselbalch curve at the same temperature. The curve of $[\theta]_{227}$ undergoes little change in the pH range of the β-disordered chain transformation, as already pointed out. The increase in negative values at low pH values occurs in the same range in which aggregation takes place (Figure 4). Values of $[\theta]_{203}$, on the other hand, increase considerably in the pH range of the conformational transition. In summary, although the pH profiles of $[\theta]_{227}$ and $s_{20,w}$ for sample 1 are insensitive to the occurrence of the conformational interconversion, the infrared spectra, the potentiometric titration data, and the pH dependence of $[\theta]_{203}$ indicate that concerted changes occur which may be ascribed to the β disordered transition.

The conformational transition of the remaining sample of $(Tyr)_n$, sample 2, whose DP is intermediate between those of samples 1 and 3, was also studied. The CD spectra in the region of the ^{1}L$_a$ band undergo no striking change in band shape as the pH is lowered. This resembles the pattern found for sample
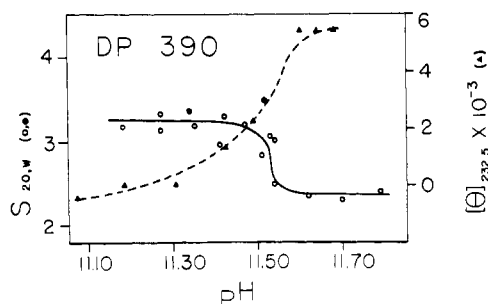
FIGURE 6: pH dependence of properties of sample 2. The sedimentation coefficient in 0.01 M sodium phosphate (○) and in 0.01 M TMAP (●) and the molar ellipticity in the region of the ^1L_a band (▲) are shown.
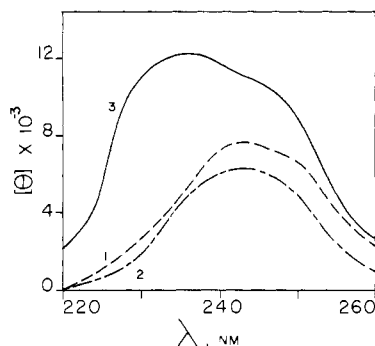

FIGURE 7: CD spectra of poly(L-tyrosine) samples at low ionization: (- - -) sample 1 in 0.01 M sodium phosphate, pH 11.54; (- - -) sample 2 in 0.01 M sodium phosphate, pH 11.41; (—) sample 3 in 0.01 M TMAP, pH 11.53.

1. Slight changes in band shape were observed, which were maximal at 232.5 nm. The pH dependence of $[\theta]_{232.5}$ and of $s_{20,w}$ for this sample are shown in Figure 6. As the pH is lowered, the values of $s_{20,w}$ increase concomitantly with the change observed in the values of $[\theta]_{232.5}$. These phenomena are ascribed to the occurrence of the β disordered chain transformation in this sample. It is interesting that in spite of the relatively high DP of sample 2 its CD spectra manifest the same pattern as found with sample 1, whose DP is much lower.

The data presented thus far demonstrate that there are two classes of β pleated-sheet structure generated by poly(L-tyrosine) in aqueous solution which are dependent upon the molecular weight. Class I, exemplified by samples 1 and 2, is characterized by the absence of negative ellipticity at 227 nm and relatively low values of the sedimentation coefficient (see Discussion). Class II, represented by sample 3, exhibits an intense negative CD band at 227 nm and has a relatively large value of $s_{20,w}$.

In order to demonstrate that this distinction is not artifactual, conditions were sought which would produce a reversible transformation between the properties exhibited by these two classes in the same sample. As a possible approach to this problem, it has been noted that the electrostatic potential in the ordered state depends weakly on α for sample 1, indicative of a low surface charge density, while the dependence for sample 3 is stronger, characteristic of a high charge density (McKnight and Auer, 1976). One might try to capitalize on this observation by seeking to increase the electrostatic repulsion between the fixed charges in sample 3, so that it might convert to the structure of sample 1 with the lower charge density. Lowering the ionic strength in order to decrease the shielding of the potential at the electrical double layer is not sufficient, however. The ratio of concentrations of counterions to fixed charges, with the dilute solutions of $(Tyr)_n$ used here
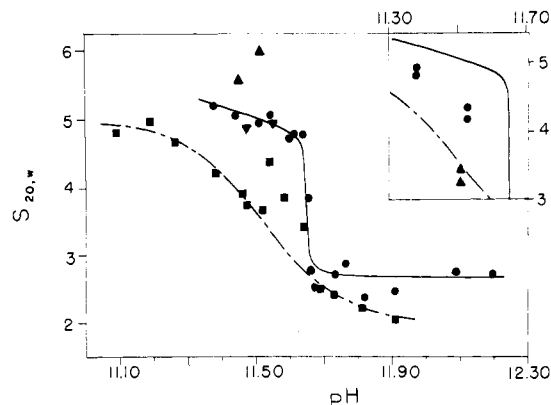

FIGURE 8: pH dependence of the sedimentation coefficient of sample 3: (●) 0.01 M sodium phosphate; (▲) 0.1 M sodium phosphate; (▼) 0.001 M sodium phosphate; (■) 0.01 M TMAP. *Inset*, reversibility of treatment with TMAP. The smooth curves are redrawn from and have the same meaning as in the main figure: (▲) 0.01 M sodium phosphate + 0.01 MTMAP after titration from the disordered state to pH 11.47; (●) after dialysis from this mixed medium to 0.01 M sodium phosphate and adjustment to pH 11.48 (see caption to Figure 9).

at the low values of α prevalent in the β form, remains large enough to be considered under the case of excess salt (Alexandrowicz and Daniel, 1963). Accordingly, values of $s_{20,w}$ for sample 3 obtained at 0.002 M Na^+ show no distinction from the trend found at 0.02 M Na^+ (Figure 8), although a significant decrease would be expected if a transformation to class I had occurred.

TMAP Medium. An alternative way to alter the shielded electrostatic potential of the polyelectrolyte is to change the identity of the counterion in order to affect the degree of counterion immobilization. It may be supposed that larger, more diffuse cations which have no chemical affinity for the oxide moiety of the tyrosinate anion would be immobilized to a lesser degree than sodium (for example, see Morawetz, 1965), thereby leading to less shielding and a higher potential at the double layer. In this spirit, experiments were carried out on sample 3 in TMAP, 0.01 M in phosphate. As the pH is decreased to the range where the ordered state is found, the CD spectrum manifests the characteristics of the low-molecular-weight class in the region of the ^1L_a band, although the intensity which develops is considerably greater than that of samples 1 and 2 in sodium medium (Figure 7). At still lower pH, the extremum at 235 nm remains unchanged, while the shoulder at 245 nm, due to tyrosinate residues, decreases in amplitude (not shown).

The pH dependence of the sedimentation coefficient of sample 3 in TMA and in sodium is compared in Figure 8. In TMA medium, a fast-sedimenting component clearly identifiable as aggregated material was observed at the lowest pH value, 11.09, where α is quite low. This portion of the boundary was included in the procedure used in evaluating $s_{20,w}$. It is likely that rapidly equilibrating aggregation may be occurring at slightly higher pH values as well, although no resolved boundaries were apparent. Lower values of $s_{20,w}$ would be observed in the absence of aggregation. Corrections to the observed values of $s_{20,w}$ in TMA in order to account for the change in the immobilized counterion from sodium to TMA were estimated by using the rationale outlined in Patton and Auer (1975). The partial molar volume of the TMA cation was obtained from that of TMA bromide (Wen and Saito, 1964) by subtracting the contribution of bromide (Pedersen, 1958). This correction would decrease the sedimentation coefficients in the region of the β form by about 5%. For these reasons, the
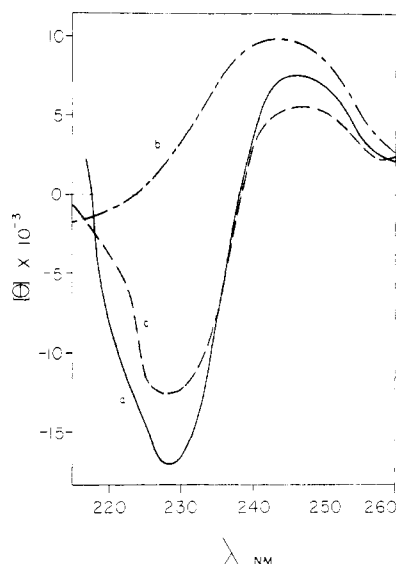
FIGURE 9: CD spectra of sample 3 upon exposure to and subsequent removal of TMA: (a) 0.01 M sodium phosphate and 0.01 M TMAP, pH 11.47; (b) the same solution after raising the pH to 12.2 and lowering again to pH 11.47; (c) the solution of spectrum 2 was dialyzed against two changes of 0.01 M sodium phosphate, pH 11.8, raised to pH 12.2, and lowered to pH 11.48.

value of $s_{20,w}$ characteristic of the β form is probably considerably lower than illustrated. The breadth of the transition region in TMA is greater than 0.5 pH unit (Figure 8). This is broader than that detected for sample 1 from the potentiometric titration (McKnight and Auer, 1976, and Figure 4) and the CD titration (Figure 5) and is considerably broader than observed for sample 2 (Figure 6). This finding indicates that the transition in TMA has a relatively low degree of cooperativity.

The pH dependence of $s_{20,w}$ in sodium medium is given in Figure 8 in order to contrast with the results in TMA. Three points are worthy of note. First, the value of $s_{20,w}$ in the β state in sodium is greater than that found for TMA and may be significantly larger in light of the corrections for aggregation and for the partial molar volume of the TMA counterion just discussed. Second, the transition is very sharp on the pH scale, comparable to that observed in 0.16 M Na$^+$ (Patton and Auer, 1975). This is characteristic of a conformational transition having a high degree of cooperativity. Finally, the midpoint of the transition in sodium occurs at a higher pH than in TMA, consistent with the notion that the shielding due to sodium is greater than that due to TMA.

In 0.2 M Na$^+$, the values of $s_{20,w}$ are found to be greater than found in 0.02 M Na$^+$ at the same pH (Figure 8), while the CD spectra are essentially unchanged.

Our CD and sedimentation results suggest that the transfer of sample 3 from sodium to TMA has indeed brought about a transformation in the nature of the pleated-sheet structure formed from that of class II to that of class I. These results could be interpreted, however, as indications that TMAP actually induces chain scission, leading to a decrease in the molecular weight for the sample. In order to demonstrate that this is not the case, a solution of sample 3 in 0.01 M sodium phosphate at a pH at which the ordered state prevails was brought to 0.01 M in TMAP. The CD spectrum obtained just after adding TMAP is shown as curve a in Figure 9 and is the same as that found prior to the addition (not shown). The sample was now taken back to high pH to generate the disordered state and then returned to the initial pH in the range of the ordered state.

The CD spectrum (Figure 9b) acquires the shape characteristic of class I, just as found for sample 3 in simple TMA medium (Figure 7). This manipulation demonstrates that the failure to bring about the change in CD spectral form upon the initial addition of TMAP is due to a kinetic barrier rather than to an unfavorable change in free energy of the ordered state. The solution of sample 3 in the mixed medium was then dialyzed against two changes of 0.01 M sodium phosphate, pH 11.8. Upon lowering the pH of the resulting solution into the range of the ordered state, the CD spectrum characteristic of class II reappears (Figure 9c), although the amplitude is slightly weaker.

Sedimentation coefficients were also determined during the course of the experiment just outlined and are included in Figure 8 (inset). The value of $s_{20,w}$ in mixed Na–TMA medium after generating the CD spectrum typical of class I (Figure 9b) falls from the range characteristic of class II in pure sodium to the range found for this sample in pure TMA (class I). Upon dialyzing back to pure sodium (cf. Figure 9c), the values of $s_{20,w}$ return to higher values, approaching the magnitudes found in pure sodium at the same pH values. The results of these experiments demonstrate that by both spectroscopic and hydrodynamic criteria the interconversion of sample 3 between the behavior typical of classes I and II is reversible. Therefore, the change observed upon transfer from sodium to TMA media cannot be ascribed to artifacts arising from chain scission. The inability to return quantitatively to the original values of molar ellipticity and $s_{20,w}$ may be due to the preferential adsorption of the longest polymer chains to the dialysis tubing. These are the ones most prone to generate the properties characteristic of class II.

As a final control, the properties of sample 2 in TMA medium were examined in the ordered state. The sedimentation coefficients were the same as found in sodium medium (Figure 6). The CD spectra in TMAP retain the same form as in sodium medium, but the amplitudes are considerably enhanced (not shown). A similar increase in intensity was noted for sample 3. These results indicate that the simple act of changing the counterion of poly(L-tyrosine) from sodium to TMA cannot be responsible for the effects observed with sample 3.

Discussion

The Antiparallel β Pleated-Sheet Conformation. The infrared spectra obtained at low ionization for both samples 1 (this work) and 3 (Patton and Auer, 1975) manifest the amide I bands at about 1630 and 1695 cm^{-1}. In analyses of the infrared spectra of poly(amino acids) in ordered conformations, these peaks have been identified as the $\nu(\pi, 0)$ and $\nu(\pi, \pi)$ components, respectively, of the amide I band in the antiparallel β pleated sheet (Miyazawa, 1960; Chirgadze and Nevskaya, 1976a,b; Moore and Krimm, 1976a,b). The parallel chain β structure is predicted to exhibit no band in the region above 1650 cm^{-1} (Chirgadze and Nevskaya, 1976a) nor is it expected that chain segments with orientations mixed between parallel and antiparallel senses would lead to the observed splitting. It may therefore be concluded that the ordered state found with samples 1 and 3 is the antiparallel β pleated-sheet conformation, in agreement with previous studies of this material (Patrone et al., 1970; Senior et al., 1971; Chirgadze and Nevskaya, 1976a). There is no reason to doubt that sample 2 follows suit. These results justify our interpretation of the potentiometric titration experiments on samples 1 and 3 exclusively in terms of β-disordered chain transitions (McKnight and Auer, 1976).

Two Classes of β Structure in Poly(Tyr). In this work and

in our preceding paper (McKnight and Auer, 1976) evidence has been adduced for the existence of a molecular weight dependence in the properties of poly(L-tyrosine) in the intramolecular β form in sodium-containing aqueous solution. This behavior is summarized in Table II, in which the properties characteristic of each class and the distribution of the three samples among them are shown. Sample 2 was not studied extensively because it is the one noted in McKnight and Auer (1976) to be 3 to 5% racemized. Its properties in class I appear normal, insofar as they were investigated, but the decreased optical purity may be responsible for the unusual observation that this sample, whose DP is only 10% smaller than that of sample 3, clearly falls into the category of class I.

Hydrodynamic Models for the Particles of Classes I and II. One of the most striking distinctions evident between the two classes is the difference in the experimental frictional ratios, f/f_{min}, listed in Table III. These were determined from sedimentation coefficients (Tanford, 1961), using a value for the partial specific volume of 0.71 cm³/g (Cohn and Edsall, 1943). Because of the large distinctions observed, no corrections were applied for the estimated effects of the degree of hydration or the degree of counterion binding on the results (Tanford, 1961; Patton and Auer, 1975).

The experimental values were compared with the values of the frictional ratio f/f_0 calculated for various β structured particles using simple hydrodynamic models. In each case, the volume of a rectangular prism was computed from the degree of polymerization, assuming a residue repeat along the polypeptide chain of 3.45 Å, an interchain spacing of 4.75 Å (Fraser and Macrae, 1973), and an intersheet distance of 14.4 Å (Patton and Auer, 1975). The extended chain model assumes a single β-structured strand in the form of a rigid rod, with no hydrogen bonding to a polypeptide mate. The hairpin loop and three-stranded sheet models assume one and two hairpin turns (such as the β turn), respectively, to yield two and three strands, respectively, hydrogen bonded to each other in antiparallel fashion. The folded-sheet models assume that single β sheets formed by n strands of the polypeptide chain, each *l* residues long, have been folded additionally in such a way as to stack two sheets together to form a two-layered particle. All these hypothetical particles were modeled by prolate ellipsoids of revolution having the same volume as the rectangular prism. The semimajor axis *a* was set equal to one-half the overall length of the prism in order to calculate the axial ratio *a/b*. In addition, square, single-layered (i.e., unfolded) sheets were approximated by determining the dimensions of a cylinder of equal volume and thickness and then setting the semimajor axis of an oblate ellipsoid of revolution equal to the radius of the cylinder. The values of f/f_0 were calculated from Perrin's equations for translational frictional ratios (Tanford, 1961). No attempt was made to account for the additional complexity introduced by the twisting of the plane of the β strand and the β sheet (Chothia, 1973).

Table III presents the frictional ratios f/f_0 predicted for various particle shapes assumed for samples 1, 2, and 3 and compares them with the experimental values of f/f_{min}. Two entries appear for sample 1, corresponding to sedimentation coefficients and the molecular weight determined in recent work, and in our earlier studies, respectively. For the samples belonging to class I, characterized by high values of f/f_{min}, only highly asymmetric particles yield values of f/f_0 which are in accord with the values of f/f_{min}. Sample 1 appears to form either a hairpin loop or an extended chain which, instead of being completely rigid, probably flexes in the manner of the wormlike chain (Kratky and Porod, 1949). The result for sample 2 is best explained in terms of a three-stranded β structure of those

TABLE II: Two Classes of Behavior of Poly(L-tyrosine) in the β Pleated-Sheet Conformation, 0.01 M Sodium Phosphate.

sample	class I		class II
	1	2	3
$\Delta S^{a,b}$	−3.85		−3.42
$\Delta pK_a/\Delta\alpha^{a,c}$	1.11		1.75
transition^{a,d}	broad	broad	sharp
$[\theta]_{227}$	~0	~0	intense neg
$[\theta]_{201}$	moderate pos		intense pos
$s_{20,w}$	1.31 ± 0.19	3.19 ± 0.12	5.07 ± 0.11

^{a} Data from potentiometric titrations (McKnight and Auer, 1976). ^{b} ΔS for disordered chain to β transition. ^{c} Slope of curve of pK_{app} vs. the degree of ionization in the region of the β form. ^{d} Breadth of disordered chain to β transition plotted vs. pH.

models considered. It is clear that a compact structure, such as an open square sheet, is not in accord with our data.

In our earlier work at high ionic strength on a sample similar to sample 3, the model of a square sheet folded once over on itself was found to explain an experimental value of f/f_{min} = 1.09 quite satisfactorily (Patton and Auer, 1975). Experiments with sample 3 were repeated under similar conditions. Much the same results were found (Figure 8 and Table III). For the folded sheet models it was assumed that an *n*-stranded sheet is folded parallel to the strand axis to yield a double-layered particle *l* residues long and *n*/2 strands wide. The best fit is for a folded rectangular sheet. A folded square sheet is acceptable, while an open square sheet predicts a larger value of f/f_0 which nevertheless falls within the bounds determined by the standard deviation in f/f_{min}. Our earlier results (Patton and Auer, 1975) had a lower standard deviation and may be considered a valid basis upon which to exclude the latter model A CD spectrum typical of class II obtained under these conditions supports this point of view. It is evident that extended or hairpin structures need not be considered in this case.

At low ionic strength, sample 3 exhibits a higher frictional ratio f/f_{min} than at high ionic strength (Table III). Since the CD spectrum retains the intense negative extremum at 227 nm (Figure 1), it is plausible to consider a folded model for this case. A particle of rather asymmetric proportions was found to accord well with the experimental result (Table III). The models conceived for the high ionic strength study of sample 3 apply here as well and should be studied for comparison. The entry in Table III for the folded rectangular sheet is written as if seven to eight strands fold to a double-layered structure having three to four strands each by breaking an entire strand equivalent of hydrogen bonds. It is considered more likely that an open sheet of three to four strands having 118 residues each forms first. It then folds along a line perpendicular to each strand by forming β turns. This conjecture is based on our finding that long strands are prevalent at low ionic strength in samples 1 and 2. If two processes such as these do indeed occur, they could account for the two-step first-order kinetics observed for the disordered to β transformation at 0.16 M sodium or potassium (Auer and Patton, 1976).

Correlation of Properties with Proposed Structures. Table II contrasts a number of properties of the two classes of particle. Let us consider whether they are consistent with the hydrodynamic models. First, in the potentiometric titrations of samples 1 and 3 it was found that both samples had the same value for ΔH per residue for the disordered β transition, but that the value of ΔS for sample 1 was more negative than for sample 3 (Table II; McKnight and Auer, 1976). From model studies it has been proposed that the formation of hydrophobic interactions between aromatic moieties is essentially athermal

TABLE III: Frictional Ratios of Poly(L-tyrosine) in the β Pleated Sheet Conformation.

model[a]	a/b	l residues	n strands	f/f_0	f/f_{min}	$[Na^+]$, M	sample
extended chain (P)	30.8	102	1	2.38			
hairpin loop (P)	10.9	51	2	1.59	1.94 ± 0.33	0.02	1[b]
square sheet (O)	2.14	12	9	1.05			
extended chain (P)	50.5	167	1	2.96			
hairpin loop (P)	17.9	84	2	1.91	2.31 ± 0.39	0.02	1[c]
square sheet (O)	2.74	15	11	1.09			
hairpin loop (P)	41.7	195	2	2.72			
3-stranded sheet (P)	22.7	130	3	2.10	1.95 ± 0.21	0.02	2
square sheet (O)	4.18	23	17	1.18			
folded rectangular sheet (P)	2.70[d]	33	14	1.09[d]			
folded square sheet (P)	1.78	25	18	1.03	1.09 ± 0.15	0.16	3
square sheet (O)	4.49	25	18	1.19			
Folded rectangular sheet (P)	6.42[d]	59	7–8	1.34[d]	1.34 ± 0.03	0.02	3

[a] Rectangular prisms are modeled by ellipsoids of revolution having the same volume as the prism: P, prolate ellipsoid; O, oblate ellipsoid. Folded models have singly folded sheets yielding double-layered particles. All others are open, single-layered particles. [b] Later measurements, done toward the end of this project (DP = 104). [c] Early measurements, done at time of the work by McKnight and Auer (1976; DP = 167). [d] The value of a/b was adjusted so that f/f_0 was identical to f/f_{min}.

($\Delta H \approx 0$) but that ΔS is positive (Frank and Evans, 1945; Kauzmann, 1959). An extended or looped structure (at the time of the titration studies sample 1 had a DP of 167) should offer minimal opportunity for hydrophobic interactions between tyrosine side chains, while in a folded structure (sample 3) all the side chains that meet in between the two layers (i.e., one-half the total) become completely sequestered from the aqueous medium, thus leading to an increase in entropy with no change in enthalpy. This is consistent with observation.

Second, the folded structure is predicted to have a higher surface charge density because it is assumed that the residues in the interior of the fold, out of contact with solvent, must be un-ionized. In the extended or looped structures, on the other hand, all the residues are susceptible of ionization, leading to a much more diffuse charge density. This would account for the stronger dependence of the electrostatic potential on the degree of ionization found for sample 3 than for sample 1. Third, the formation of a folded structure leads to noncovalent interactions between more residues, which are proliferated in more dimensions, than is the case for extended or looped structures. Therefore, a higher degree of cooperativity is predicted for sample 3 than for sample 1. This too is consistent with observation.

Finally, the CD spectra found in class I differ from those of class II, with lower intensity at 201 nm and no band arising at 227 nm in samples 1 and 2, in contrast to intense bands at both wavelengths in sample 3. While no predictions of optical activity for the β form of $(Tyr)_n$ have been made, the opportunity for coupling interactions between chromophoric side chains exists in the folded structure postulated for sample 3, which could not occur in the extended or looped structures proposed for samples 1 and 2. This coupling could give rise to the greater CD intensities observed with sample 3.

The Open Structure in TMA Medium. Upon transfer of sample 3 from sodium to TMA media its properties change in significant ways. First, the CD spectrum in the ordered state changes from that characteristic of class II to that found in class I. Second, the sedimentation coefficient at low ionization decreases (see Results), leading to an increase in f/f_{min}. Quantitative estimates of f/f_{min} are not possible because of the lack of a plateau in the value of $s_{20,w}$ at low ionization in Figure 8. Third, the order–disorder transformation as monitored by the pH dependence of $s_{20,w}$ becomes quite broad. All these considerations are consistent with an open-sheet structure for sample 3 in TMA medium. Thus, the transfer of sample 3 from sodium to TMA brings about a transformation of the β structure from a folded, compact structure to an open, single-layered conformation. This transformation has been shown to be reversible.

Conclusion

At low solute concentration and low ionization, poly(L-tyrosine) forms an intramolecular antiparallel β structure. The detailed conformation adopted depends critically on molecular weight and the chemical identity of the counterion. Under most conditions, the particle adopts a highly anisotropic shape, comprised of one, two, or a few long strands assembled into single sheets. When the chain length is great enough and the counterion is sodium, the particle is far more compact, having a larger number of shorter strands folded into (at least) a two-layered structure. This extension of the β pleated sheet from the normal two dimensions into three represents what may be the first demonstration of intramolecular tertiary structure in a β-forming system, one as simple as a homopoly(amino acid). As such, poly(Tyr) constitutes an excellent model system for the study of tertiary structure in native proteins, since the conditions leading to this state are so readily controlled. Further studies in this direction are intended.

Acknowledgment

We thank Mr. Paul Ritter for excellent technical assistance in portions of this work.

References

Alexandrowicz, Z., and Daniel, E. (1963), *Biopolymers 1*, 447–471.

Auer, H. E., and Patton, E. (1976), *Biophys. Chem. 4*, 15–21.

Chirgadze, Yu. N., and Nevskaya, N. A. (1976a), *Biopolymers 15*, 607–625.

Chirgadze, Yu. N., and Nevskaya, N. A. (1976b), *Biopolymers 15*, 627–636.

Chothia, C. (1973), *J. Mol. Biol. 75*, 295–302.

Cohn, E. J., and Edsall, J. T. (1943), Proteins, Amino Acids and Peptides as Ions and Dipolar Ions, Reinhold, New York, N.Y., p 372.

Conio, G., Patrone, E., and Salaris, F. (1971), *Macromolecules* *4*, 283–288.

Frank, H. S., and Evans, M. W. (1945), *J. Chem. Phys. 13*, 507–532.

Fraser, R. D. B., and MacRae, T. P. (1973), Conformation in Fibrous Proteins, Academic Press, New York, N.Y., pp 218–246.

Hartman, R., Schwaner, R. C., and Hermans, J., Jr. (1974), *J. Mol. Biol. 90*, 415–429.

Hooker, T. M., Jr., and Schellman, J. A. (1970), *Biopolymers 9*, 1319–1348.

Kauzmann, W. (1959), *Adv. Protein Chem. 14*, 1–63.

Kratky, O., and Porod, G. (1949), *Recl. Trav. Chim. Pays–Bas 68*, 1106–1122.

McKnight, R. P., and Auer, H. E. (1976), *Macromolecules 9*, 939–944.

Miyazawa, T. (1960), *J. Chem. Phys. 32*, 1647–1652.

Moore, W. H., and Krimm, S. (1976a), *Biopolymers 15*, 2439–2463.

Moore, W. H., and Krimm, S. (1976b), *Biopolymers 15*, 2465–2483.

Morawetz, H. (1965), Macromolecules in Solution, 1st ed, Interscience, New York, N.Y., pp 360–361.

Patrone, E., Conio, G., and Brighetti, S. (1970), *Biopolymers 9*, 897–910.

Patton, E., and Auer, H. E. (1975), *Biopolymers 14*, 849–869.

Pedersen, K. O. (1958), *J. Phys. Chem. 62*, 1282–1290.

Senior, M. B., Gorell, S. L. H., and Hamori, E. (1971), *Biopolymers 10*, 2387–2404.

Tanford, C. (1961), Physical Chemistry of Macromolecules, Wiley, New York, N.Y., pp 326–343.

Wen, W. Y., and Saito, S. (1964), *J. Phys. Chem. 68*, 2639–2644.

Probes of the Mechanism of Zymogen Catalysis[†]

John D. Lonsdale-Eccles,[‡] Hans Neurath, and Kenneth A. Walsh*

ABSTRACT: Trypsinogen and chymotrypsinogen hydrolyze *p*-nitrophenyl esters of several peptides and *tert*-butyloxy-carbonyl amino acids. The best substrate found for chymotrypsinogen was Boc-Ala-ONp and for trypsinogen Z-Gly-Hyp-Gly-ONp. Comparison of the kinetic parameters indicates that in the zymogens the catalytic site is distorted and reduced in effectiveness by about two orders of magnitude, in addition to a 10 000-fold decrease in catalysis due to a distortion of the primary substrate binding site (Kerr, M. A., Walsh, K. A., & Neurath, H. (1976) *Biochemistry 15*, 5566). Using Boc-Ala-ONp as substrate and certain aldehydes and borates as inhibitors, the zymogens were tested for the integrity of the "oxyanion hole", but these results were largely inconclusive. Probes for the secondary binding sites indicated their presence in trypsinogen and their absence in chymotrypsinogen.

Kinetic studies of the catalytic activity of zymogens have indicated that the major change in the zymogen/enzyme transformation involves the development of a primary binding site (also called the tosyl hole or P_1 binding site; Gertler et al., 1974; Kerr et al., 1975). Since the zymogen reacts more slowly than the enzyme with methanesulfonyl fluoride (Morgan et al., 1972), and since acyl-zymogens deacylate more slowly than acyl-enzymes (Kerr et al., 1975), it was suggested that in the zymogen the oxyanion hole is also distorted (Kerr et al., 1976). Similar conclusions have been drawn from studies employing a variety of physical and chemical techniques (Robillard & Schulman, 1974; Freer et al., 1970; Birktoft et al., 1976; Hanai, 1976; Fehlhammer et al., 1977; Reeck et al., 1977; Porubcan et al., 1977). Past kinetic studies have been restricted to the use of pseudo-substrates or active-site titrants, e.g., *p*-nitrophenyl-*p*'-guanidinobenzoate, and consequently may be called into question because the peculiar molecular geometry of these compounds may render them unsuitable for the detection of the subtle rearrangements which have been observed by x-ray studies (see Kerr et al., 1976). To overcome this possible re-striction, we have explored in the present work aminoacyl esters as potential substrates for trypsinogen and chymotrypsinogen. The effect of the length of both the P_1 side chain and the peptide chain itself upon the catalytic activity of these zymogens was studied. In addition, by utilizing a new substrate to monitor catalysis, we have compared zymogens and their enzymes in their reactivity toward various ligands which interact with the secondary binding sites and/or the oxyanion hole.

Materials and Methods

Once recrystallized bovine trypsinogen, lyophilized bovine trypsin, 3× crystallized bovine chymotrypsinogen, and α-chymotrypsin were products of Worthington Biochemical Corp. The esters Boc-Ala-ONp[1] and Ac-Ala-Ala-Ala-OMe and the inhibitor phenylboronic acid were products of Sigma. The compounds Ac-Ala-Ala-AzaAla-ONp and Z-Gly-Leu-Ala chloromethyl ketone were gifts from Dr. J. C. Powers (Georgia Institute of Technology). The esters Z-Ser-Gly-Gly-ONp and Z-Gly-Hyp-Gly-ONp were prepared for us by Professor T. Wieland (Heidelberg). Elastatinal, a peptide al-

[1] Abbreviations used: Boc, *tert*-butyloxycarbonyl; Z, benzyloxycarbonyl; Abu, α-aminobutyric acid; Nva, norvaline; Hyp, hydroxyproline; AzaAla, azaalanine (N^1-methyl carbazate); Dip-F, diisopropyl fluorophosphate; DIP, diisopropyl phosphoryl; NPGB, *p*-nitrophenyl *p*'-guanidinobenzoate; -ONp, *p*-nitrophenyl ester; -OMe, methyl ester; Pipes, piperazine-*N,N*'-bis(2-ethanesulfonic acid).

© 1978 American Chemical Society